Preparation and application of modified activated carbon for effective removal of phosphorus from glyphosate by-product salt

Qisheng Wu*, Jie Zhang, Sen Wang

College of Materials Science and Engineering, Yancheng Institute of Technology, Yancheng 224051, China,
emails: qishengwu@ycit.cn (Q. Wu), 3021116592@qq.com (J. Zhang), 12700697 36@qq.com (S. Wang)

ABSTRACT

Glyphosate is a non-selective, residue-free insecticidal herbicide, and its byproduct salts obtained through evaporation and concentration have high phosphorus content, thus preventing resource utilization. In this paper, cerium-aluminum-modified activated carbon (Ce/Al-AC) adsorbent was synthesized by loading cerium-aluminum into the interior and surface of activated carbon using the oil bath method with activated carbon as the raw material. Phosphorus removal using activated carbon composite adsorbent and the influences of pH, initial waste salt concentration, modified activated carbon addition, and adsorption time on the phosphorus extraction effectiveness of modified activated carbon were investigated in a controlled variable manner. As part of the characterization of the adsorbent, scanning electron microscopy, X-ray diffraction, and Fourier-transform infrared spectroscopy were performed. The experimental results show that under the conditions of 10 g/L glyphosate waste salt solution, the initial phosphorus concentration of 32.67 mg/L, the amount of adsorbent addition of 10 g/L, pH 7, and the adsorption time of 180 min, the phosphorus removal rate of unmodified activated carbon is 36.2%. In contrast, the rate of modified activated carbon can reach more than 99%. With the modified activated carbon adsorbent, a pH range of 3–11 was effective for adsorption, with the best adsorption performance observed at neuter pH. Phosphorus removal followed Langmuir (R^2 = 0.921) models. The theoretical adsorption capacity reached 8.13 mg/g. The total phosphorus content was decreased to below 0.5 mg/L. This study demonstrates that modified activated carbon has potential value in the treatment of glyphosate byproduct salt and high-salinity wastewater.

Keywords: Glyphosate; Activated carbon; Composite adsorbent; Phosphorus removal; Regeneration

1. Introduction

Phosphorus is indispensable nourishment in the growth of organisms. With the rapid development of industry and agriculture, which industrial processing and agricultural runoff produce wastewater containing phosphorus, most of the wastewater containing phosphorus cannot be effectively used because of the high phosphorus content, and when the water body contains excessive phosphorus, it will eutrophicate the water body, leading to a large number of algae breeding and the death of aquatic animals in the water body [1], which poses a serious threat to the ecosystem. The process of producing glyphosate also produces a large amount of phosphorus-containing wastewater.

Glyphosate, also known as N-(phosphonomethyl) glycine, is generally used in genetically modified crops because of its high efficiency, broad-spectrum and low toxicity, and glyphosate herbicide is also one of the most representative herbicides in the world [2–4], with the chemical formula $C_3H_8NO_5P$. The chemical structure of glyphosate is indicated in Fig. 1a. Glyphosate is generally prepared by the glycine-dimethyl phosphite method, The process of glyphosate

* Corresponding author.

waste salt generation is shown in Fig. 1b, because the difficulty of recycling leads to a quantity of alkaline mother liquor being discharged, which is considered as an agricultural pollutant due to its persistence and hazard [5,6]. In their studies, experts have found the occurrence of glyphosate in water and soil and its possible contamination of our habitat [7,8]. Therefore, it is necessary to effectively treat the glyphosate wastewater before its discharge to make its wastewater harmless. The by-products of glyphosate contain high phosphorus content, which is difficult to utilize. Therefore, phosphorus removal has become the key to the utilization of glyphosate by-product resources. Currently, known methods for phosphorus removal include photocatalytic degradation [9], membrane separation [10], electrolysis [11], adsorption [12], and biological treatment [13]. The traditional chemical precipitation method for phosphorus removal is simple, but the addition of excessive phosphorus removal reagent may lead to secondary contamination of the solution. The biological treatment technology is generally used in low-concentration saline treatment, and the cost of photocatalytic degradation method is too high. Among them, adsorption method has been widely used because of its simple operation, no special facility requirements, low energy consumption and high adsorption speed.

The selection of the adsorbent has a great influence on the adsorption properties. The materials used as adsorbents are usually characterized by large specific surface region and high porosity, such as diatomaceous earth [14], zeolite [15], palygorskite [16], natural polymers and biopolymers (usually polysaccharides such as chitosan and its derivatives) [17], red mud [18], and activated carbon, etc. Compared with activated carbon, other adsorbent materials tend to have poor acid resistance, poor mechanical strength, and lack versatility [19–22], Therefore, activated carbon has been widely used as an adsorption material [23–25], but the adsorption capacity of activated carbon for phosphorus is small and it does not provide specific interaction with phosphate ions, a series of modifications are needed to enhance the phosphorus removal performance of activated carbon. In recent years, modified activated carbon has been widely used in the field of water treatment. Activated carbon after heat treatment can adsorb acid dye [26] and carbon dioxide [27]. Also, can be through acid modification to improve the efficiency of carbon dioxide adsorption [28]. Impregnated with several metal oxides (Ni, V, Fe and Ce) of palm shell activated carbon can be used in adsorption gas SO_2 and NO_x [29], through surface reduction treatment can be used as adsorption binary aromatic solute [30]. Many metal salts can react with phosphate to form precipitation, so as to remove phosphate from water, and use iron, aluminum, calcium and other metal compounds to modify phosphorus has become a research focus in recent years. However, there are relatively few research reports on phosphorus removal by high concentrations of glyphosate by-product salts.

In this study, cerium chloride and aluminum chloride were used as raw materials for activated carbon modification, and the modified activated carbon was prepared by the oil bath method. The calcined treated glyphosate waste salt was configured into a certain concentration of waste salt solution. The effects of solution pH variation, waste salt concentration variation, modified activated carbon adsorbent addition variation and adsorption time variation on the removal of phosphorus from glyphosate waste salt by modified activated carbon were investigated. The adsorption mechanism of modified activated carbon was studied using a series of characterization tools [X-ray diffraction (XRD), scanning electron microscopy (SEM), Fourier-transform infrared spectroscopy (FTIR) and mapping], adsorption kinetics and adsorption isotherm analysis.

2. Experimental part

2.1. Reagents

Glyphosate by-product salt was provided by Hubei Xingfa Chemical Group Co., Ltd., in China. Activated carbon was supplied by Sinopharm Chemical Reagent Co., Ltd., (Shanghai, China). Pure analysis grade chemicals, including cerium chloride ($CeCl_3 \cdot 6H_2O$) was supplied by Shanghai Macklin Biochemical Co., Ltd., (Shanghai, China), hexahydrate and aluminum chloride ($AlCl_3 \cdot 6H_2O$), sodium hydroxide (NaOH) from Jiangsu-based Wuxi City Sheng Chemical Co., Ltd., (Jiangsu, China). Hydrochloric acid (HCl) from Nanjing Chemical Reagent Co., Ltd., (Nanjing, China).

2.2. Calcination treatment

The glyphosate byproduct salt was placed in a muffle furnace, and the sample was subjected to calcination at a temperature of 550°C for 2 h and taken out after natural cooling. Organic phosphorus in glyphosate byproduct salt was converted to inorganic phosphorus [31].

2.3. Preparation of the composite adsorbent

Weigh 0.71 g of $CeCl_3 \cdot 6H_2O$ and 0.48 g of $AlCl_3 \cdot 6H_2O$ into a 150 mL volumetric flask, pour 100 mL of distilled water to dissolve them, and get the cerium-aluminum mixed solution; 2 g of activated carbon were added to the solution containing cerium and aluminum and used an ultrasonic cleaner at a frequency of 40 Hz to sonicate for
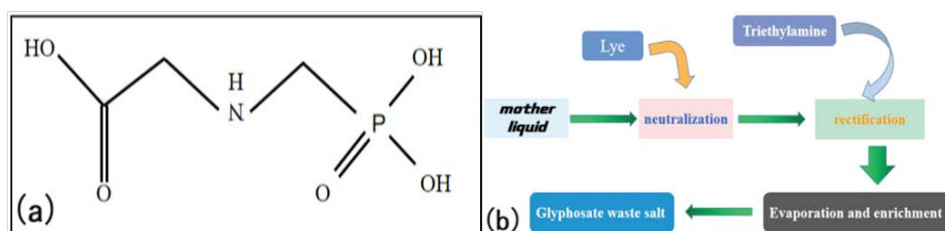
Fig. 1. (a) Chemical structure of glyphosate and (b) process of glyphosate waste salt generation.

30 min to distribute the activated carbon in the mixed solution evenly. We adapted the pH to a range of 10–11 using sodium hydroxide. The mixture underwent magnetic stirring in an oil bath maintained at 80°C for 12 h, filtered, put into a drying oven at 75°C and dried until the weight was constant to obtain cerium-aluminum modified activated carbon (Ce/Al-AC). The preparation and adsorption process of altered activated carbon is shown in Fig. 2.

2.4. Material characterization

The material structure was characterized using XRD analysis performed with a Panalytical X'Pert3Powder instrument provided by Panalytical, The Netherlands. CuKα radiation was employed, and the diffraction angles covered a range from 5° to 80°. SEM images were obtained using a Thermo Fisher Nova Nano SEM 450 operating at 15 kV to observe the morphology and grain size of the samples. FTIR spectroscopy using a Nicolet NEXUS-670 instrument from the USA was utilized to evaluate changes in the functional groups of the materials before and after modification. Phosphorus content was analyzed using a rapid tester designed for total phosphorus measurements (6B-70B, Sheng Aohua Technology Co., Ltd.).

2.5. Adsorption experiment

10 g of calcined glyphosate by-product salt was placed in a 1,000 mL beaker, dissolved by adding a certain amount of distilled water, and poured into a 1l volumetric flask. The volume was fixed at 1 L to obtain a 10 g/L spent salt solution. 50 mL of this wastewater was then treated using a magnetic mixer with an oscillation frequency of 160 rpm under various adsorption conditions, including different phosphorus mass concentrations, pH values, varying adsorbent dosages, and adsorption times. After filtration, determination of total phosphorus concentration using total phosphorus rapid tester. Then, find the phosphorus removal efficiency rate and adsorption capacity are calculated [31,32]:

$$\eta = \frac{\left(C_0 - C_e\right)}{C_0} \times 100\% \qquad (1)$$

$$q_e = \frac{\left(C_0 - C_e\right) \times V}{m} \qquad (2)$$

where C_0 and C_e denote the mass concentration of phosphorus before and after phosphorus removal, respectively, in mg/L; V denotes the wastewater volume, in L; m is the amount of adsorbent added, in g. η denotes the removal rate of phosphorus, %; q_e denotes the adsorption capacity of phosphorus by the adsorbent, in mg/g.

2.6. Regeneration experiment

Weigh 0.5 g of Ce/Al-AC phosphorus removal agent and add it into a 50 mL solution containing 10 g/L of glyphosate byproduct salt. Magnetic stirring for 3 h to reach adsorption balance and to acquire the adsorption ability q_e (mg/g). Then, after phosphorus removal, the modified

Fig. 2. Preparation of modified activated carbon and adsorption process.

activated carbon was transferred to 50 mL of ultrapure water, 0.1, 0.2 and 0.3 mol/L sodium hydroxide solutions and sonicated for 30 min. Wash and dry, conduct the experiment on phosphorus removal to determine the adsorption capacity q_d (mg/g) after regeneration. The formula to calculate the regeneration rate was:

$$\text{Reg} = \left[\frac{q_d}{q_e}\right] \times 100\% \qquad (3)$$

where q_d refers to the adsorption ability after regeneration(mg/g); q_e represents the adsorption ability of the phosphorus removal agent before regeneration (mg/g).

3. Results and discussion

3.1. Characterization of the composite adsorbent

Fig. 3a shows the XRD characteristic peaks of AC, Al-AC, Ce-AC, and Ce/Al-AC. These peaks around 22° are distinct peaks of carbon materials, showing that both AC samples have good carbonization performance. After cerium modification, the modified adsorbent exhibited new peaks at 28.7°, 32.9°, 47.2°, 56.3°, and 76.9°, which matched the characteristic peaks of cerium oxide (JCPDF Card No. 34-0394), indicating the successful loading of cerium in the form of cerium oxide onto the activated carbon. However, no changes in the XRD pattern between aluminum-modified materials and the original material could be observed. Probably, the amount of successful doping was relatively small, which had no impact on the activated carbon structure [32].

Fig. 3b shows the FTIR spectra of AC and Ce/Al-AC composite materials. The O–H stretching vibration peak was observed at 3,732 cm⁻¹, while the carbon-based absorption peak was at 1,624 cm⁻¹. Ce/Al-AC samples showed a stretching vibration peak at 1,056 cm⁻¹ corresponding to the C–O–C bond [33], and the peaks for C–H bending vibrations were at 826 and 736 cm⁻¹. The findings indicate that the surface of the adsorbent composite exhibits oxygen-containing functional groups exhibiting hydrophilic properties. These results were consistent with XRD analysis, which showed successful doping of CeO_2 particles onto the surface of AC.

Fig. 4a and b shows the SEM images of unmodified AC and Ce/Al-AC, respectively. A comparison reveals that the

unmodified activated carbon has more pores and a relatively smooth surface. After cerium-aluminum modification, the accumulation of cerium-aluminum oxides leads to a rough and irregular surface. The diffraction images of various elements in Fig. 4c–f further confirm the presence of oxides.

3.2. Different phosphorus removal agent phosphorus removal results

A comparison of the adsorption properties of AC with different modifiers is shown in Fig. 5. Phosphorus removal experiments were conducted on four types of adsorbents: activated carbon raw material, Al-AC, Ce-AC, and Ce/Al-AC. Each of the four adsorbents was taken at 0.5 g and placed in a 50 mL solution of 10 g/L glyphosate waste salt, followed by stirring for adsorption experiments. As indicated in Fig. 5, raw activated carbon removes 29% of phosphorus. Modification with Ce or Al can enhance the phosphorus removal rate of activated carbon. It has been shown that Ce/Al-AC can remove 99.45% of phosphorus.

3.3. Removal of phosphorus in batch experiments

3.3.1. Effect of solution pH

As shown in Fig. 6a and b, when the incipient pH of the by-product salt solution of glyphosate increases from 3

to 11, the modified activated carbon shows little change in adsorption ability. The best adsorption effect is observed when the solution is neutered, with a maximum adsorption
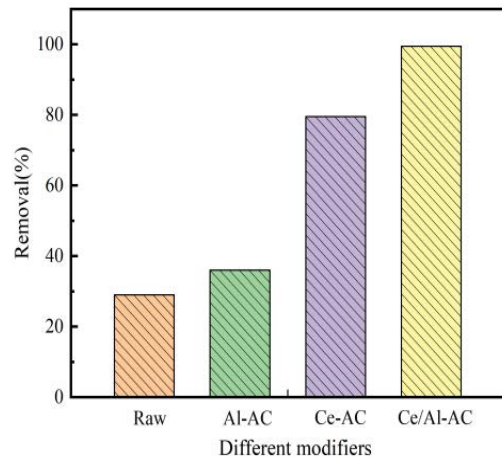
Fig. 5. Phosphorus removal rates affected by different modifiers (initial total phosphorus concentration of 32.67 mg/L, volume of 50 mL, contact time of 180 min, temperature of 25°C, and adsorbent dose of 10 g/L).
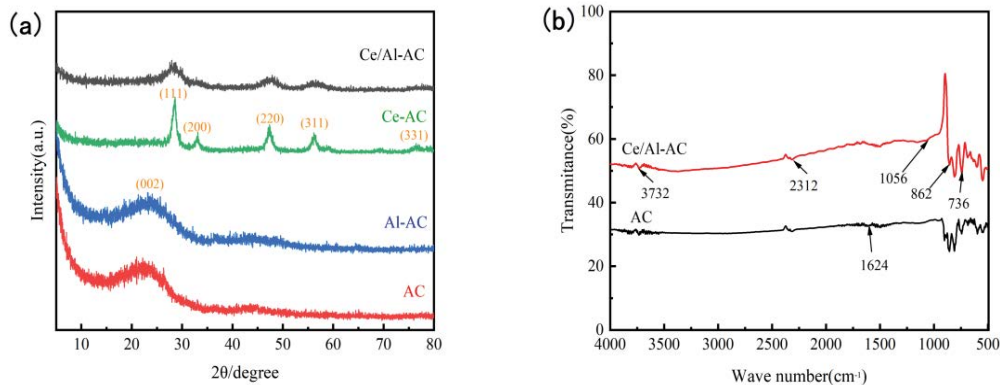
Fig. 3. (a) X-ray diffraction profile of AC and Ce/Al-AC composite adsorbent. (b) Fourier-transform infrared spectroscopy of AC and Ce/Al-AC.
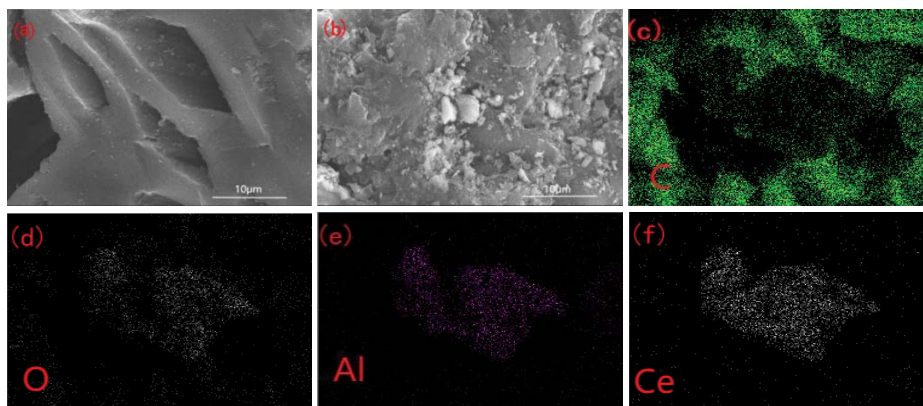
Fig. 4. Scanning electron microscopy images of AC (a) and Ce/Al-AC (b), elemental mapping images of carbon (c) and oxygen (d), aluminium (e) and cerium (f).

capacity of 2.98 mg/L and the highest removal rate of 99.8%, while the lowest removal rate is still at 99.3%. Therefore, when using Ce/Al-AC as a phosphorus adsorbent, it is not necessary to deliberately adjust the initial solution pH to a certain value or range.

3.3.2. Effect of salt concentration

Glyphosate by-product salt is calcined, and the waste salt obtained is configured into different concentrations of glyphosate waste salt solution. As shown in Fig. 7a and b, with the concentration of waste salt increases, the Ce/Al-AC was less effective in removing phosphorus, while the adsorption capacity increased, with a maximum value of 6.4 mg/L. Due to the addition of a fixed amount of modified activated carbon as a phosphorus adsorbent, the increasing concentration of by-products from glyphosate results in higher total phosphorus content. However, due to the limited number of adsorption sites, some phosphorus molecules could not match with adsorption sites. As a result, the rate of phosphorus removal decreases. Increasing phosphorus concentration in the solution dispersed more phosphorus around the modified activated carbon. Therefore, Ce/Al-AC is able to adsorb more effectively.

3.3.3. Effect of adsorbent dose amount

As shown in Fig. 8a and b, the phosphorus removal rate increases with Ce/Al-AC adsorbent addition, but the adsorption capacity decreases. When the addition amount was 0.7 g, the phosphorus removal rate arrived at 99.71%, and the adsorption ability decreased to 2.13 mg/L. This is because with the increase of activated carbon phosphorus removal agent addition, the adsorption point of action increased and the phosphorus content in the waste salt solution was fixed, making the phosphorus adsorption more adequate.

3.3.4. Effect of contact time

Fig. 9a and b show the phosphorus removal efficiency of Ce/Al-AC adsorbents as a function of adsorption time. The adsorbent rapidly adsorbed within 30 min, with a removal rate exceeding 70%. When the adsorption time was increased to 120 min, the phosphorus adsorption by Ce/Al-AC adsorbent decreased. When the adsorption time reached 180 min, the phosphorus removal rate by the Ce/Al-AC adsorbent remained stable, and the adsorption capacity reached 2.98 mg/L.
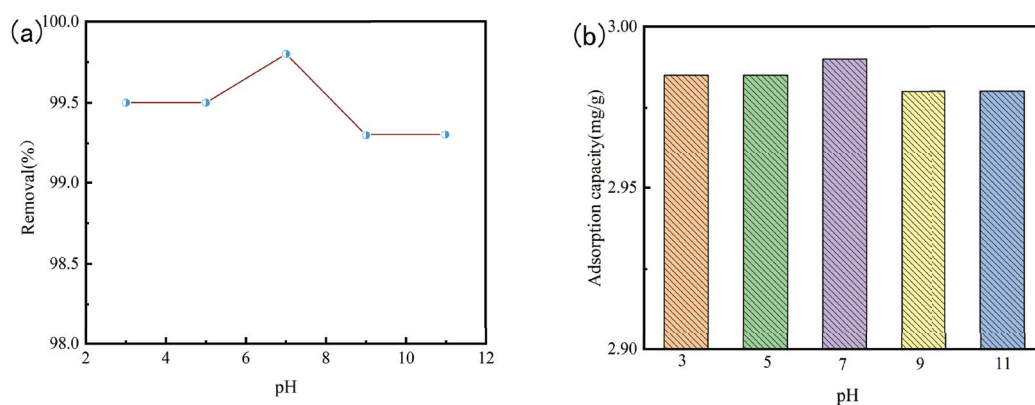
Fig. 6. Effect of pH on phosphorus removal from Ce/Al-AC composite adsorbent (a) and adsorption capacity (b) (initial total phosphorus concentration of 32.67 mg/L, volume of 50 mL, contact time of 180 min, temperature of 25°C, and adsorbent dose of 10 g/L).
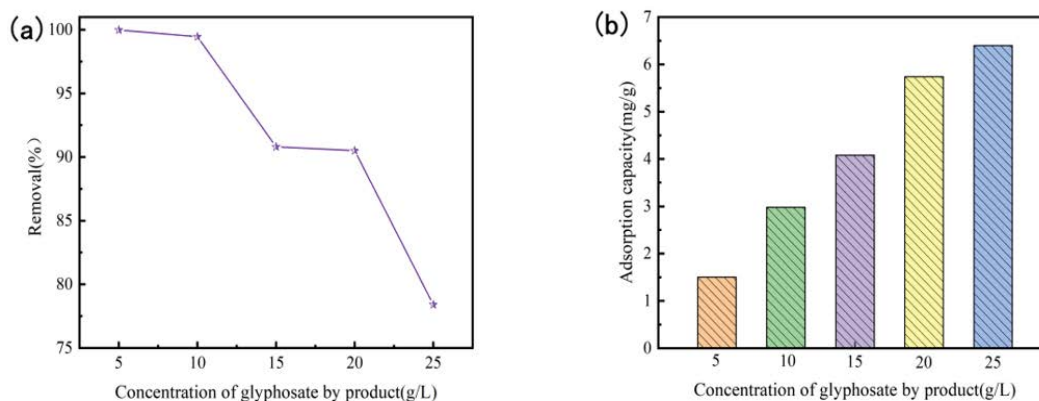
Fig. 7. Effect of salt concentration on phosphorus removal rate (a) and adsorption capacity (b) (volume 50 mL, adsorption time 180 min, temperature 25°C, and adsorbent dose 10 g/L).
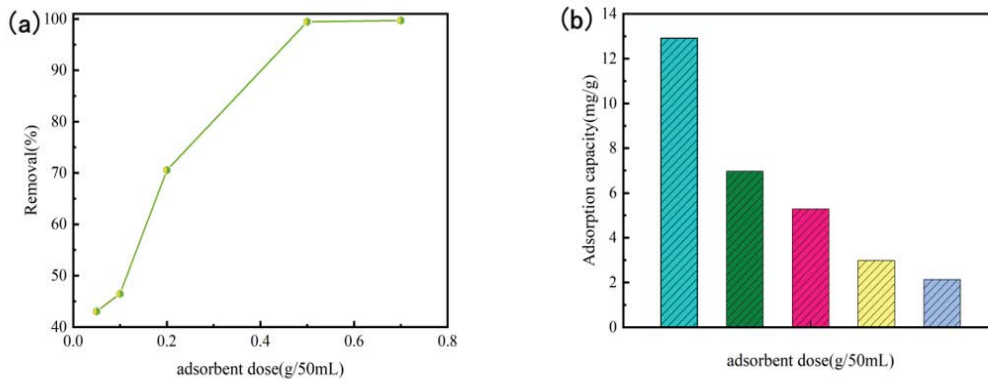
Fig. 8. Effect of Ce/Al-AC addition on phosphorus removal rate (a) and adsorption capacity (b) (initial phosphorus concentration of 32.67 mg/L, volume 50 mL, contact time 180 min, and temperature 25°C).
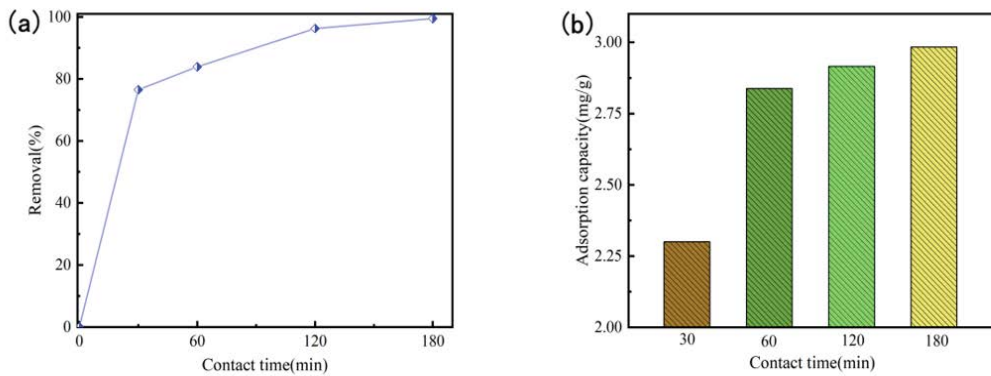
Fig. 9. Effect of contact time on the phosphorus removal rate (a) and adsorption capacity(b) (initial phosphorus concentration of 32.67 mg/L, volume of 50 mL, temperature of 25**C**, and adsorbent dose of 10 g/L).

3.4. Mechanism for phosphorus removal in Ce/Al-AC

3.4.1. Adsorption kinetics of Ce/Al-AC

A pseudo-first-order and pseudo-second-order kinetic model was used to study the adsorption kinetics of Ce/Al-modified activated carbon. Additionally, to analyze adsorbent diffusion, the particle intraparticle diffusion model was applied [34], the following adsorption kinetic equation:

$$\ln\left(q_e - q_t\right) = \ln q_e - k_1 t \tag{4}$$

$$\frac{t}{q_e} = \frac{1}{k_2^2 q_e^2} + \frac{1}{q_t} \tag{5}$$

$$q_t = k_D t^{0.5} + C \tag{6}$$

Figs. 10a, b and 11 depict the results of the three kinetic models, and the simulated parameters are shown in Table 1. The pseudo-second-order kinetic model exhibited an R^2 value of 0.999, which was closer to 1 than the other two kinetic models, indicating that in the present study, Ce/Al-AC was adsorbed by chemical means [35]. From Fig. 11, intraparticle diffusion can be found to include two main stages: liquid film diffusion stage and diffusion toward adsorption sites step. The stage time ranges were approximately

$5.5 < t^{0.5} < 11.0$ min$^{0.5}$ (first stage) and $11.0 < t^{0.5} < 15.5$ min$^{0.5}$ (second stage) [36].

3.4.2. Adsorption isotherms

This study employed three different isothermal adsorption models to discuss the adsorption mechanism of phosphorus removal using modified Ce/Al-AC adsorbent.

$$\frac{1}{q_e} = \frac{1}{K_L q_m C_e} + \frac{1}{q_m} \tag{7}$$

$$\ln q_e = \ln K_F + \frac{1}{n} \ln C_e \tag{8}$$

$$q_e = \left(\frac{RT}{b}\right) \ln A + \left(\frac{RT}{b}\right) \ln C_e \tag{9}$$

Figs. 12a, b and 13 represent three isothermal adsorption models. Compared to the R^2, results obtained from the other two isothermal adsorption models, the Langmuir simulation parameters were closer to 1, indicating that this is a monolayer adsorption-activated carbon adsorbent. Based on Langmuir simulation parameters, the theoretical adsorption of Ce/Al-AC was calculated up to 8.13 mg/g.
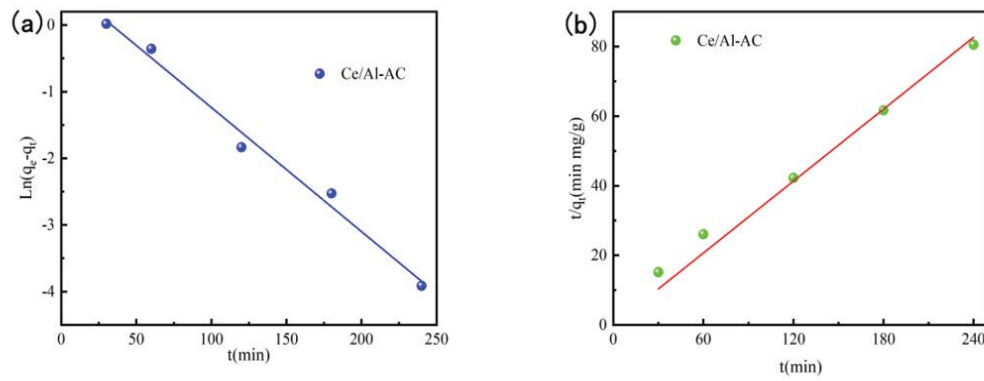
Fig. 10. Adsorption kinetics: (a) pseudo-first-order and (b) pseudo-second-order equations.

Table 1
Model constants for phosphorus adsorption by modified activated carbon based on pseudo-first-order, pseudo-second-order and intraparticle diffusion model constants

Adsorbents	$(q_e)_{exp}$ (mg/g)	Pseudo-first-order model			Pseudo-second-order model			Intraparticle diffusion model		
		K_1 (min^{-1})	q_e (mg/g)	R^2	K_2 (g/mg·min)	q_e (mg/g)	R^2	K_D	C	R^2
Ce/Al-AC	2.98	0.0186	1.868	0.989	0.03	3.094	0.999	3.453	3.21	0.958
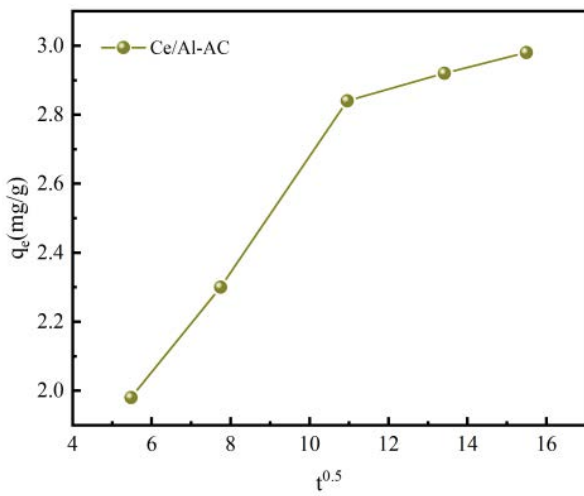
Fig. 11. Intraparticle diffusion of phosphate onto adsorbents.
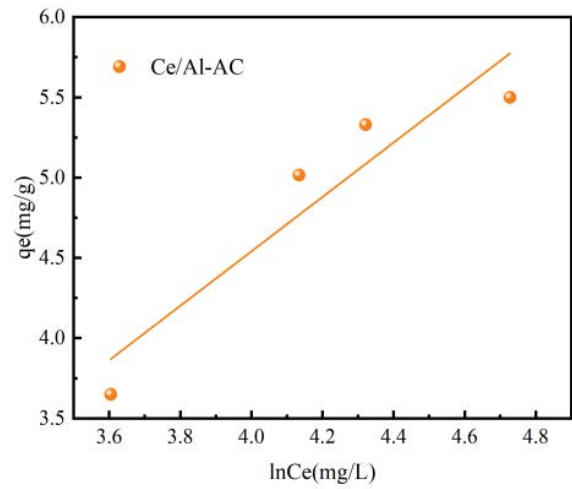
Fig. 13. Temkin model.
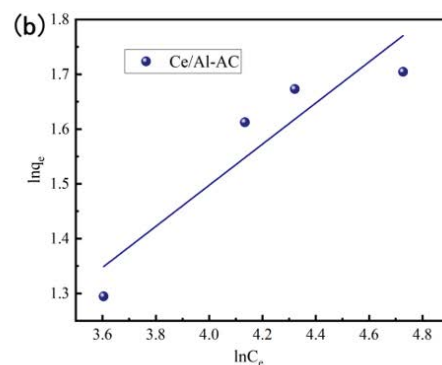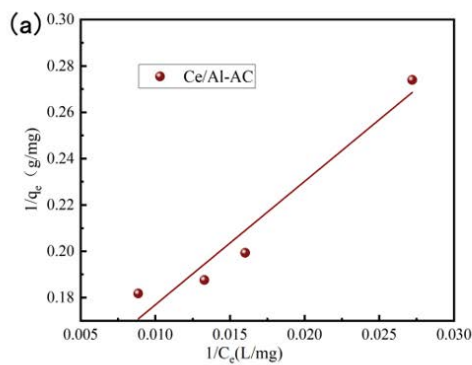
Fig. 12. Adsorption isotherm: (a) Langmuir adsorption and (b) Freundlich adsorption models.

This was close to the experimental value. The Freundlich model parameter $1/n$ ($1/n$ = 0.3756) was also used to investigate the phosphorus removal effect of Ce/Al-AC adsorbent. $1/n$ is greater than 0 and smaller than 1, indicating adsorption strength or inhomogeneity of the adsorbent surface. When $1/n$ is smaller than 1, Langmuir isotherm model well describes the adsorption process [37]. The phosphorus removal efficiency of some adsorbents was evaluated and compared with cerium-aluminum modified activated carbon. The results are summarized in Table 2.

3.4.3. Adsorption thermodynamic

The Gibbs' free energies ($\Delta G°$) can represent the [47] using Eqs. (10) and (11):

$$K_D = \frac{q_e}{C_e} \tag{10}$$

$$\Delta G° = -RT \ln K_D \tag{11}$$

Using the van't Hoff equation, the enthalpy change $\Delta H°$ (J/mol) and the entropy change $\Delta S°$ [(J/(mol·K)] are calculated by Eq. (12):

$$\ln K_D = \frac{\Delta S°}{R} - \frac{\Delta H°}{RT} \tag{12}$$

Referring to the relevant data in Table 3, the thermodynamic-related data are calculated. Gibbs' free energies ($\Delta G°$) are negative, indicating that phosphorus adsorption removal by modified activated carbon is spontaneous and favorable. $\Delta H°$ is positive, indicating that the adsorption process is an endothermic state. The entropy values tended to increase, meaning possible changes in the adsorbent surface structure [48].

3.5. Regeneration study

Desorption and regeneration experiments were carried out on the modified activated carbon after use with 0.1 mol/L sodium hydroxide, sodium carbonate, citric acid, and acetic acid, respectively. As shown in Fig. 14a, sodium hydroxide had the best regeneration effect for the activated carbon. Then, the effect of regenerating the adsorbent

Table 2
Adsorption capacity of certain adsorbents for phosphorus

Adsorbents	q_m (mg/g)
Fe-Mg-loaded activated carbon	0.76 [38]
Thermally modified sepiolite	19.49 [39]
Activated alumina	0.72 [40]
Lime mud waste	7.1 [41]
Iron tailings	10.24 [42]
Magnesium-lanthanum-modified coal gasification coarse slag	39.22 [43]
Wasted salted duck eggshells	3.32 [44]
Lanthanum modified bentonite	5.7 [45]
Lanthanum/chitosan co-modified bentonite	15.5 [46]
Cerium-aluminum modified activated carbon (present study)	8.13

Table 3
Simulation parameters of three different isothermal adsorption models

Adsorbents	Langmuir			Freundlich			Temkin		
	K_L (L/mg)	q_m (mg/g)	R^2	K_F (g/mg·min)	$1/n$	R^2	A	b	R^2
Ce/Al-AC	0.023	8.13	0.921	1.56	0.3756	0.795	9.39	1437.9	0.826
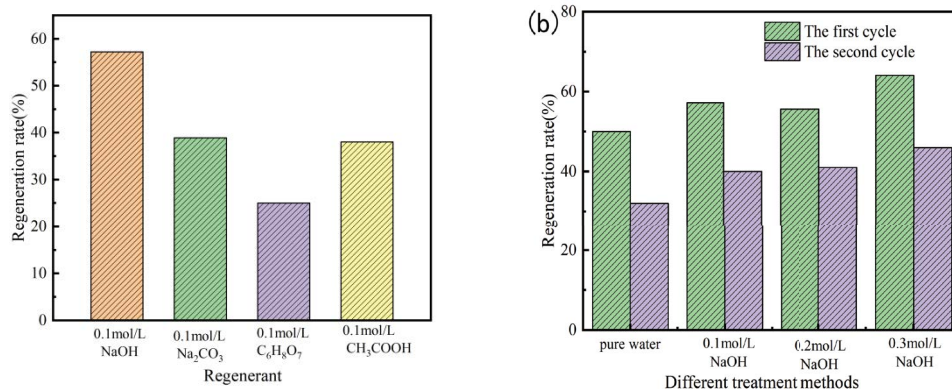
Fig. 14. (a) Effect of different regeneration reagents on the regeneration properties of modified activated carbon. (b) The impact of different concentrations of NaOH on the regeneration performance of modified activated carbon (initial phosphorus concentration of 32.67 mg/L, volume of 50 mL, adsorption time of 180 min, temperature of 25°C, and adsorbent dose of 10 g/L).

with different amounts of sodium hydroxide is shown in Fig. 14b. The adsorbent is most effectively regenerated at 0.3 mol/L NaOH concentration. With a recovery rate of up to 64.05%. The recovery rate with pure water was 51.03%. This result preliminarily demonstrates the capability of the adsorbent prepared with activated carbon to be recycled.

4. Conclusions

- In this study, cerium aluminum modified activated carbon was used to remove phosphorus from glyphosate waste salt, and the adsorbent was characterized by XRD, SEM, FTIR, etc. After measuring the TP value of glyphosate waste salt solution, the test results showed that at the addition of glyphosate with 10 g/L waste salt solution, the initial phosphorus concentration of 32.67 mg/L is 14 g/L, the adsorption time of 180 min, the total dephospination of Ce/Al-AC is the highest, reaching 99.98%. The phosphorus removal rate of activated carbon was significantly improved after modification.

- The adsorption process of phosphorus by Ce/Al-AC was a chemical adsorption, and after 120 min of contact time, the adsorption state can reach basic equilibrium. The adsorption process of Ce/Al-AC conforms to the Langmuir model, with a theoretical value of up to 8.13 mg/g and an adsorption regeneration rate of more than 60%.

Statements and declarations

No competing financial interests exist.

References

[1] Y. Dai, W. Wang, L. Lub, L. Yan, D. Yu, Utilization of biochar for the removal of nitrogen and phosphorus, J. Cleaner Prod., 257 (2020) 120–573.
[2] S. Fiorilli, L. Rivoira, G. Calì, M. Appendini, M. Concetta, M. Coïsson, B. Onida, Iron oxide inside SBA-15 modified with amino groups as reusable adsorbent for highly efficient removal of glyphosate from water, Appl. Surf. Sci., 411 (2017) 457–465.
[3] N. Botten, L.J. Wood, J.R. Werner, Glyphosate remains in forest plant tissues for a decade or more, For. Ecol. Manage., 493 (2021) 119–259.
[4] N. Lemke, A. Murawski, M.I.H. Schmied-Tobies, E. Rucic, H.-W. Hoppe, A. Conrad, M. Kolossa-Gehring, Glyphosate and aminomethylphosphonic acid (AMPA) in urine of children and adolescents in Germany - Human biomonitoring results of the German Environmental Survey 2014–2017 (GerES V), Environ. Int., 156 (2021) 106–769.
[5] Q. Tang, W. Chen, Y. Lv, S. Yang, Y. Xu, Z-scheme hierarchical Cu_2S/Bi_2WO_6 composites for improved photocatalytic activity of glyphosate degradation under visible light irradiation, Sep. Purif. Technol., 236 (2020) 1–8.
[6] D. Feng, A. Soric, O. Boutin, Treatment technologies and degradation pathways of glyphosate: a critical review, Sci. Total Environ., 742 (2020) 1–14.
[7] C.A. Villamar-Ayala, J.V. Carrera-Cevallos, R. Vasquez-Medrano, P.J. Espinoza-Montero, Fate, eco-toxicological characteristics, and treatment processes applied to water polluted with glyphosate: a critical review, Crit. Rev. Env. Sci. Technol., 49 (2019) 1476–1514.
[8] B.J. Mahler, P.C. Van Metre, T.E. Burley, K.A. Loftin, M.T. Meyer, L.H. Nowell, Similarities and differences in occurrence and temporal fluctuations in glyphosate and atrazine in small Midwestern streams (USA) during the 2013 growing season, Sci. Total Environ., 579 (2017) 149–158.
[9] H. Wu, Q. Sun, J. Chen, G.Y. Wang, D. Wang, X.F. Zeng, J.X. Wang, Citric acid-assisted ultrasmall CeO_2 nanoparticles for efficient photocatalytic degradation of glyphosate, Chem. Eng. J., 425 (2021) 130–640.
[10] X. Luo, J.B. Zhang, L. He, X.J. Yang, P.Y. Lü, Analysis of the performance and mechanism of phosphorus removal in water by steel slag, Environ. Sci., 42 (2021) 2324–2333.
[11] X.X. Wang, M. Wang, Y.X. Jia, T.T. Yao, The feasible study on the reclamation of the glyphosate neutralization liquor by bipolar membrane electrodialysis, Desalination, 300 (2012) 58–63.
[12] X. Li, L. Huang, H. Fang, M. Chen, Z. Cui, Z. Sun, D. Reible, Phosphorus adsorption by sediment considering mineral composition and environmental factors, Environ. Sci. Pollut. Res., 28 (2021) 17495–17505.
[13] Z. Fan, W. Zeng, Q. Meng, H. Liu, C. Ma, Y. Peng, Achieving partial nitrification, enhanced biological phosphorus removal and in-situ fermentation (PNPRF) in continuous-flow system and mechanism analysis at transcriptional level, Chem. Eng. J., 428 (2022) 131098, doi: 10.1016/j.cej.2021.131098.
[14] Z. Wang, Y. Lin, D. Wu, Hydrous iron oxide modified diatomite as an active filtration medium for phosphate capture, Chemosphere, 144 (2016) 1290–1298.
[15] Q.P. Cheng, H.X. Li, Y.L. Xu, S. Chen, Y.H. Liao, F. Deng, J.F. Li, Study on the adsorption of nitrogen and phosphorus from biogas slurry by NaCl-modified zeolite, PLoS One, 12 (2017) e0176109, doi: 10.1371/journal.pone.0176109.
[16] F.Q. Gan, J.M. Zhou, H.Y. Wang, C.W. Du, X.Q. Chen, Removal of phosphate from aqueous solution by thermally treated natural palygorskite, Water Res., 43 (2009) 2907–2910.
[17] H.Y. Zhu, R. Jiang, L. Xiao, G.M. Zeng, Preparation, characterization, adsorption kinetics and thermodynamics of novel magnetic chitosan enwrapping nanosized γ-Fe_2O_3 and multi-walled carbon nanotubes with enhanced adsorption properties for methyl orange, Bioresour. Technol., 101 (2010) 5063–5069.
[18] W.W. Huang, S.B. Wang, Z.H. Zhu, L. Li, X.D. Yao, V. Rudolph, F. Haghseresht, Phosphate removal from wastewater using red mud, J. Hazard. Mater., 158 (2008) 35–42.
[19] P. Zhang, Q. An, J. Guo, C.C. Wang, Synthesis of mesoporous magnetic Co-NPs/carbon nanocomposites and their adsorption property for methyl orange from aqueous solution, J. Colloid Interface Sci., 389 (2013) 10–15.
[20] W. Cheah, S. Hosseini, M.A. Khan, T.G. Chuah, T.S.A. Choong, Acid modified carbon coated monolith for methyl orange adsorption, Chem. Eng. J., 215 (2013) 747–754.
[21] R. Huang, Q. Liu, J. Huo, B. Yang, Adsorption of methyl orange onto protonated cross-linked chitosan, Arabian J. Chem., 10 (2017) 24–32.
[22] Z. Gu, B. Deng, J. Yang, Synthesis and evaluation of iron-containing ordered mesoporous carbon (FeOMC) for arsenic adsorption, Microporous Mesoporous Mater., 102 (2007) 265–273.
[23] N.F. Nejad, E. Shams, M.K. Amini, J.C. Bennett, Synthesis of magnetic mesoporous carbon and its application for adsorption of dibenzothiophene, Fuel Process. Technol., 106 (2013) 376–384.
[24] M. Valix, W.H. Cheung, G. McKay, Roles of the textural and surface chemical properties of activated carbon in the adsorption of acid blue dye, Langmuir, 22 (2006) 4574–4582.

[25] J. Goscianska, A. Olejnik, R. Pietrzak, Comparison of ordered mesoporous materials sorption properties towards amino acids, Adsorption (Boston), 19 (2013) 581–588.

[26] A.A. Attia, W.E. Rashwan, S.A. Khedr. Capacity of activated carbon in the removal of acid dyes subsequent to its thermal treatment, Dyes Pigm., 69 (2006) 128–136.

[27] A. Heidari, H. Younesi, A. Rashidi, A.A. Ghoreyshi, Evaluation of CO_2 adsorption with eucalyptus wood based activated carbon modified by ammonia solution through heat treatment, Chem. Eng. J., 254 (2014) 503–513.

[28] Y.L. Tan, Md. Azharul Islam, M. Asif, B.H. Hameed, Adsorption of carbon dioxide by sodium hydroxide-modified granular coconut shell activated carbon in a fixed bed, Energy, 77 (2014) 926–931.

[29] S. Sumathi, S. Bhatia, K.T. Lee, Selection of best impregnated palm shell activated carbon (PSAC) for simultaneous removal of SO_2 and NO_x, J. Hazard. Mater., 176 (2010) 1093–1096.

[30] F. Haghseresht, S. Nouri, G.Q.M. Lu, Effects of carbon surface chemistry and solution pH on the adsorption of binary aromatic solutes, Carbon, 41 (2003) 881–892.

[31] Q.S. Wu, M. Jiang, W.J. Zhang, Preparation of adsorbent from nickel slag for removal of phosphorus from glyphosate by-product salt, Sep. Sci. Technol., 57 (2022) 2393–2406.

[32] M. Du, Y.Y. Zhang, Z.Y. Wang, M.R. Lv, Q. Xu, Z.Q. Chen, Q.X. Wen, A. Li, La-doped activated carbon as high-efficiency phosphorus adsorbent: DFT exploration of the adsorption mechanism, Sep. Purif. Technol., 298 (2022) 121–585.

[33] J.X. Chen, K.L. Liu, M.H. Jiang, Jian Han, M.L. Liu, C.B. Wang, C.L. Li, Controllable preparation of porous hollow carbon sphere@ZIF-8: novel core-shell nanomaterial for Pb^{2+} adsorption, Colloids Surf., A, 568 (2019) 461–469.

[34] V.A. Hoang, K. Yoshizuka, S. Nishihama, Oxidative adsorption of arsenic from water environment by activated carbon modified with cerium oxide/hydroxide, Chem. Eng. Res. Des., 186 (2022) 161–173.

[35] D. Balarak, G. McKay, Utilization of MWCNTs/Al_2O_3 as adsorbent for ciprofloxacin removal: equilibrium, kinetics and thermodynamic studies, J. Environ. Sci. Health., Part A Environ. Sci. Eng. Toxic Hazard. Subst. Control, 56 (2021) 324–333.

[36] T.J. Al-Musawi, N. Mengelizadeh, O. Al Rawi, D. Balarak, Capacity and modeling of Acid blue 113 dye adsorption onto chitosan magnetized by Fe_2O_3 nanoparticles, J. Polym. Environ., 30 (2022) 344–359.

[37] J.J. Yuan, Y. Zhu, J.Z. Wang, L.P. Gan, M.Y. He, T. Zhang, P.P. Li, F.X. Qiu, Preparation and application of Mg-Al composite oxide/coconut shell carbon fiber for effective removal of phosphorus from domestic sewage, Food Bioprod. Process., 126 (2021) 293–304.

[38] P. Gao, Y. Zhang, S. Wang, Increasing the hydrophyte removal rate of dissolved inorganic phosphorus using a novel Fe-Mg-loaded activated carbon hydroponic substrate with adsorption-release dual functions, J. Environ. Manage., 313 (2022) 114998, doi: 10.1016/j.jenvman.2022.114998.

[39] P. Gao, C. Zhang, Study on phosphorus removal pathway in constructed wetlands with thermally modified sepiolite, Sustainability, 14 (2022) 12535, doi: 10.3390/su141912535.

[40] J. Diao, L. Shao, D. Liu, Y. Qiao, W. Tan, L. Wu, B. Xie, Removal of phosphorus from leach liquor of steel slag: adsorption dephosphorization with activated alumina, JOM, 70 (2018) 2027–2032.

[41] H. Vu, M. Khan, R. Chilakala, T. Lai, T. Thenepalli, J. Ahn, D. Park, J. Kim, Utilization of lime mud waste from paper mills for efficient phosphorus removal, Sustainability, 11 (2019) 1524, doi: 10.3390/su11061524.

[42] W. Li, G. Cai, K. Luo, J. Zhang, H. Li, G. Li, J. Zhang, X. Chen, F. Xie, Synthesis of magnesium-modified ceramsite from iron tailings as efficient adsorbent for phosphorus removal, Sep. Purif. Technol., 326 (2023) 124817, doi: 10.1016/j.seppur.2023.124817.

[43] B. Yang, F. Han, Y. Bai, Z. Xie, T. Shi, J. Wang, Y. Li, Phosphate removal performance and mechanism of magnesium–lanthanum-modified coal gasification coarse slag, Mater. Today Sustainability, 22 (2023) 100357, doi: 10.1016/j.mtsust.2023.100357.

[44] C. Yirong, L.-P. Vaurs, Wasted salted duck eggshells as an alternative adsorbent for phosphorus removal, J. Environ. Chem. Eng., 7 (2019) 103443, doi: 10.1016/j.jece.2019.103443.

[45] M. Zhang, Y. Zhang, X. Chen, J. Sun, X. Lu, Y. He, Y. Wang, Characteristics and mechanism of phosphate removal by lanthanum modified bentonite in the presence of dissolved organic matter, Chemosphere, 340 (2023) 139957, doi: 10.1016/j.chemosphere.2023.139957.

[46] C. Fu, Y. Li, Y. Zuo, B. Li, C. Liu, D. Liu, Y. Fu, Y. Yin, Fabrication of lanthanum/chitosan co-modified bentonite and phosphorus removal mechanism from low-concentration landscape water, Water Sci. Technol., 86 (2022) 1017–1033.

[47] F. Koochakzadeh, R. Norouzbeigi, H. Shayesteh, Statistically optimized sequential hydrothermal route for $FeTiO_3$ surface modification: evaluation of hazardous cationic dyes adsorptive removal, Environ. Sci. Pollut. Res., 30 (2022) 19167–19181.

[48] D.U. Quintela, D.C. Henrique, P.V. dos Santos Lins, A.H. Ide, A. Erto, J.L. da Silva Duarte, L. Meili, Waste of *Mytella Falcata* shells for removal of a triarylmethane biocide from water: kinetic, equilibrium, regeneration and thermodynamic studies, Colloids Surf., B, 195 (2020) 111230, doi: 10.1016/j.colsurfb.2020.111230.